Electronic Supplementary Information

Auxiliary ligands modulated trisimidazole-based coordination polymers: syntheses, structures and photoluminescent properties

Tien-Wen Tseng,*[a] Tzuoo-Tsair Luo,[a] Shou-Ju Kan,[a] and Doan Duy-An Nguyen[a]

[a] Department of Chemical Engineering and Biotechnology, National Taipei University of Technology, Taipei 106, Taiwan.

* To whom correspondence should be addressed (email: f10403@ntut.edu.tw).

Contents

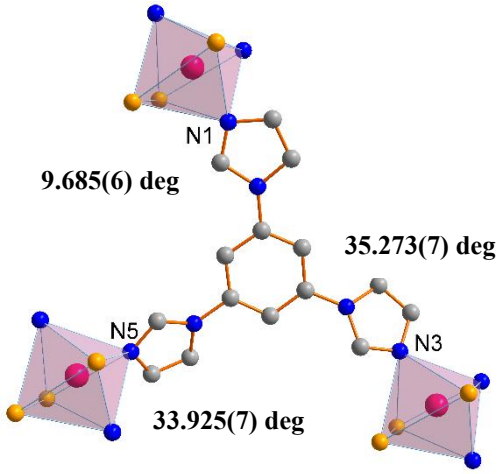

Fig. S1. The dihedral angles of the tib ligand presents in compound **1**.

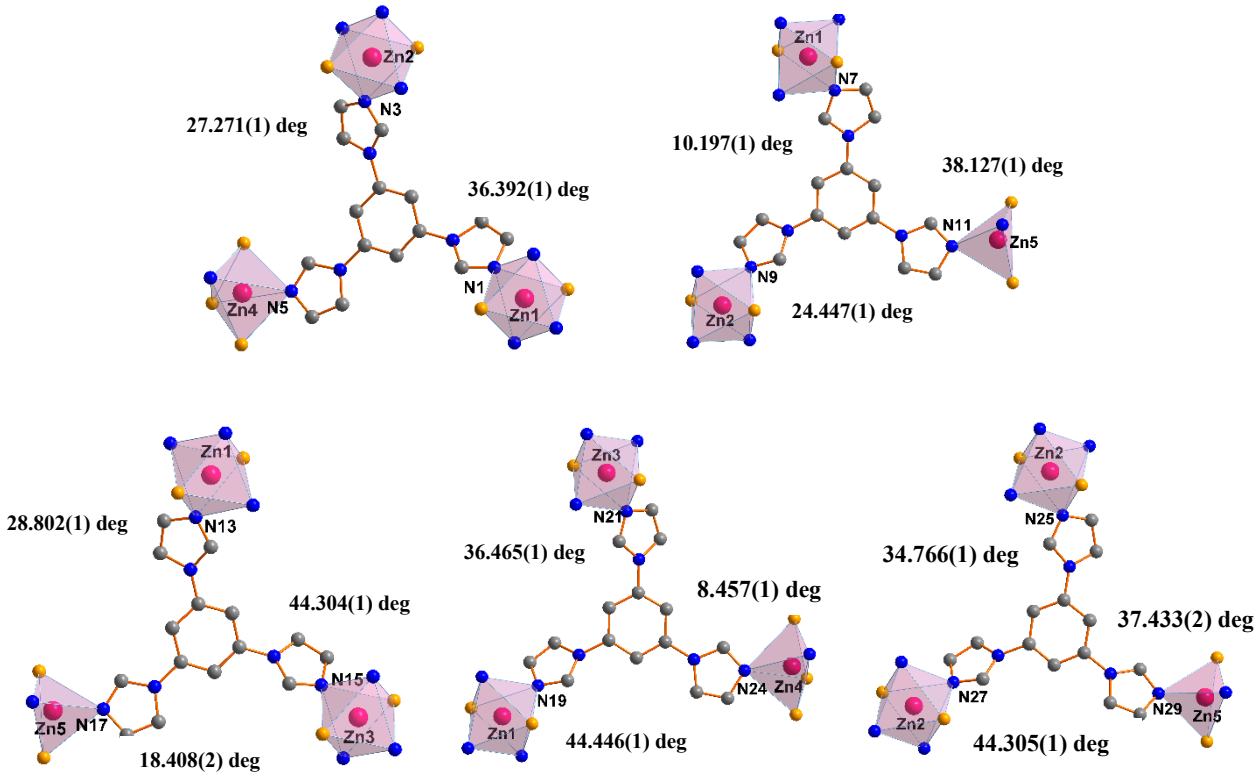

Fig. S2. Compound **2** reveals the distinct dihedral angles of the tib ligand.

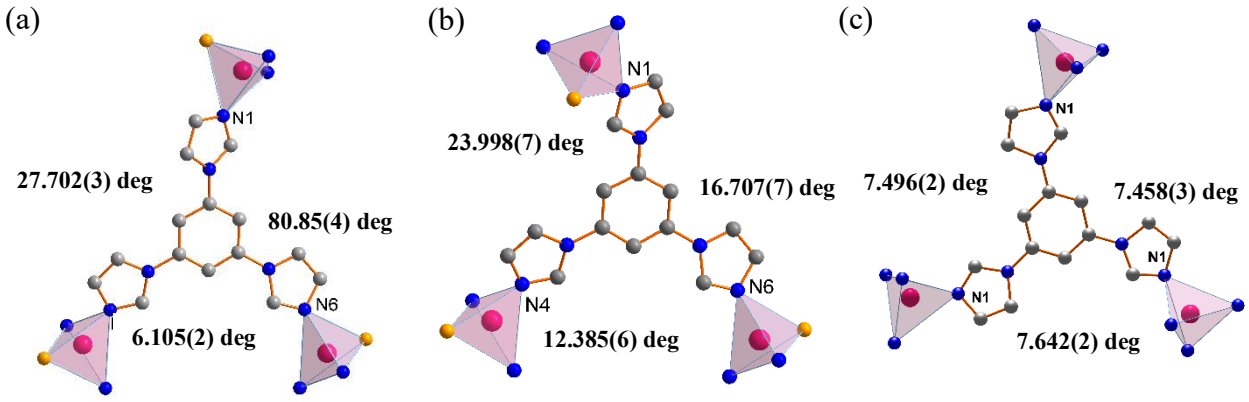

Fig. S3. Several types of dihedral angles of the tib ligand exhibited in compounds **3**–**5**: for **3** (a); for **4** (b); for **5** (c).

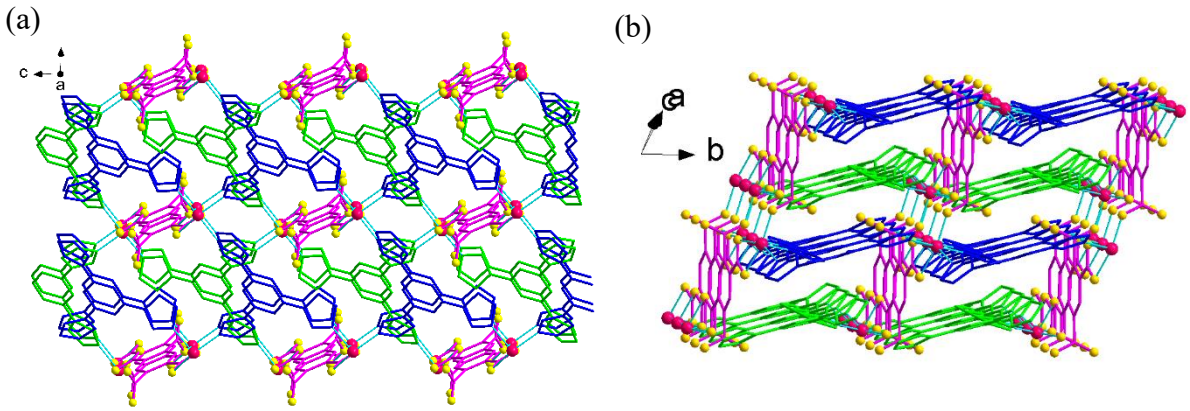

Fig. S4. The views of the 3D supramolecular structures of **1** showed in (a) and (b).

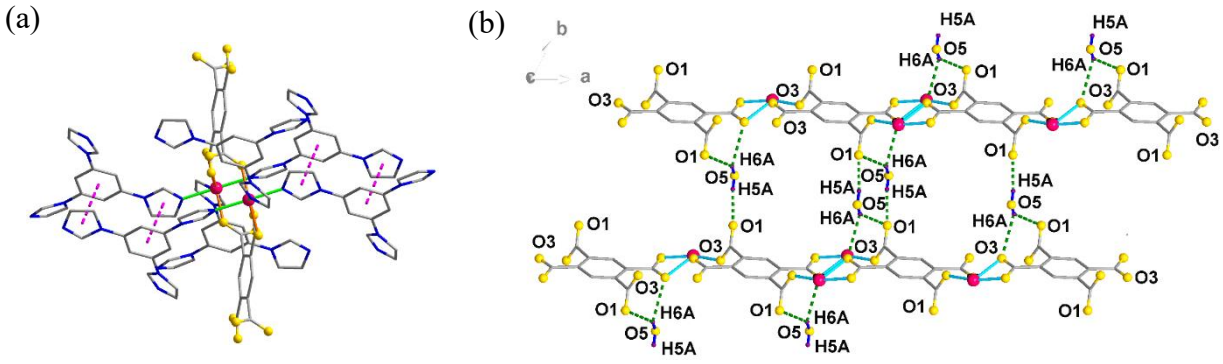

Fig. S5. Structures of **1**: (a) showing the adjacent imidazole rings of the tib ligands are regularly packed *via* π–π interactions with 3.462(1) Å (in pink dash line); (b) a view of the guest aqueous molecules are hydrogen bonded to the 1,2,4,5-benzenetetracarboxylate ($betc^{4-}$) ligands.

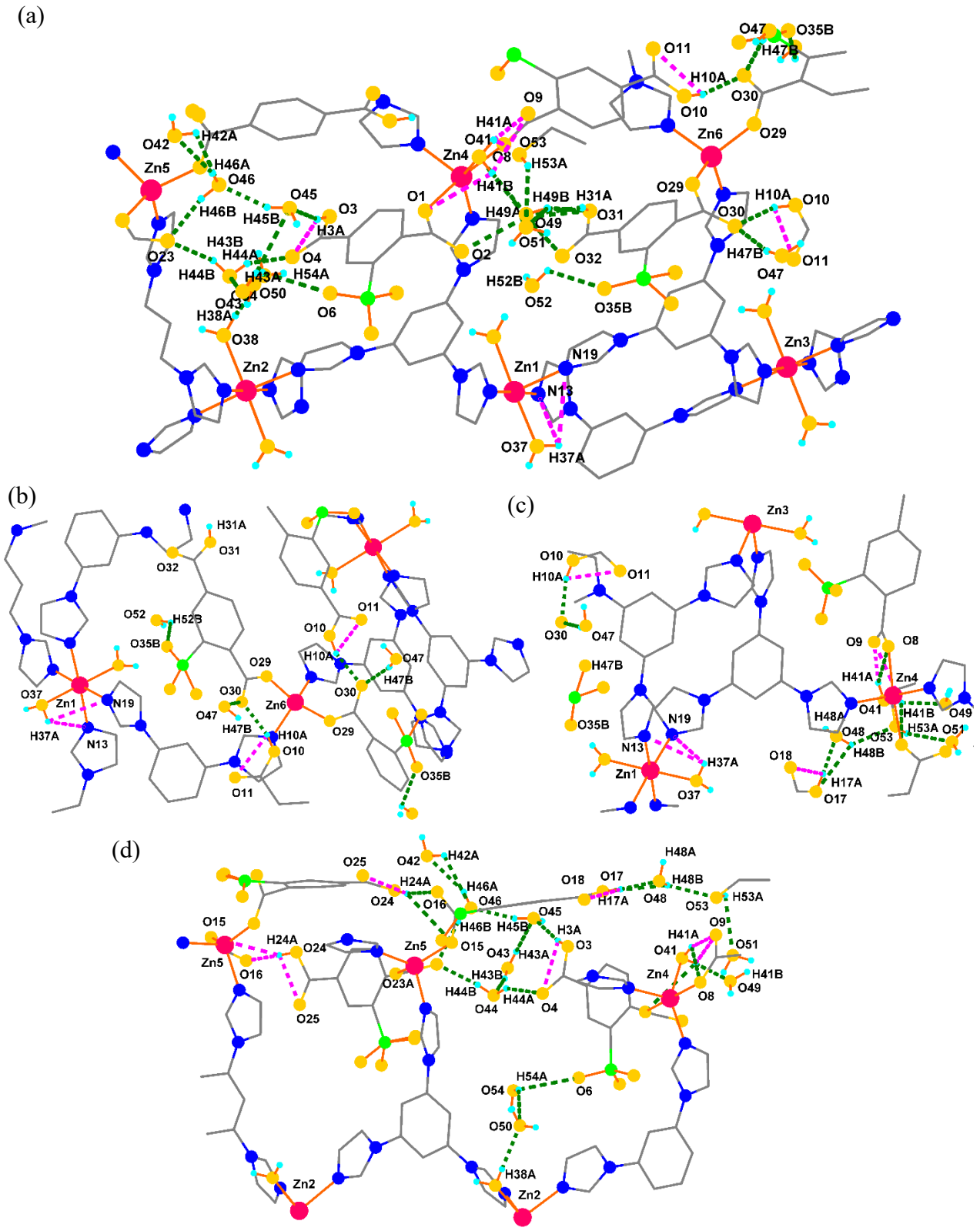

Fig. S6. The localized abundant hydrogen bonding interactions of **2** is showed in (a)–(d).

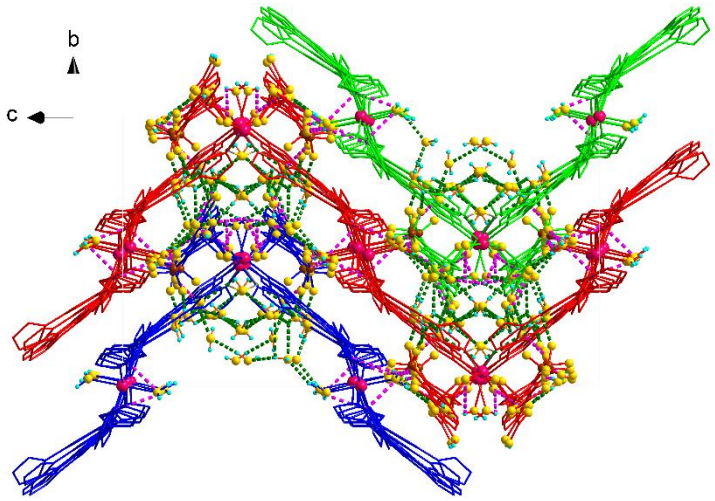

Fig. S7. The 2D wave-like networks of **2** are regularly stacked, resulting in a 3D supramolecular framework *via* the abundant hydrogen bonding interactions (in dashed lines) viewed along the *a*-axis.

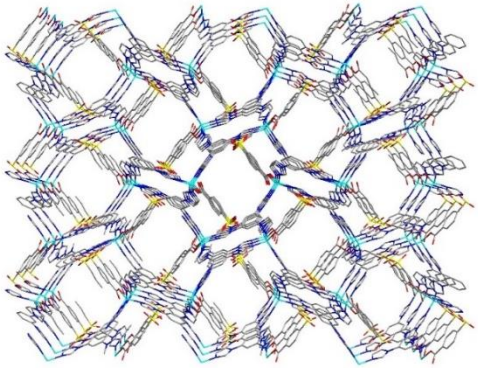

Fig. S8. A 3D packing perspective view of **3** viewed along the *a*-axis.

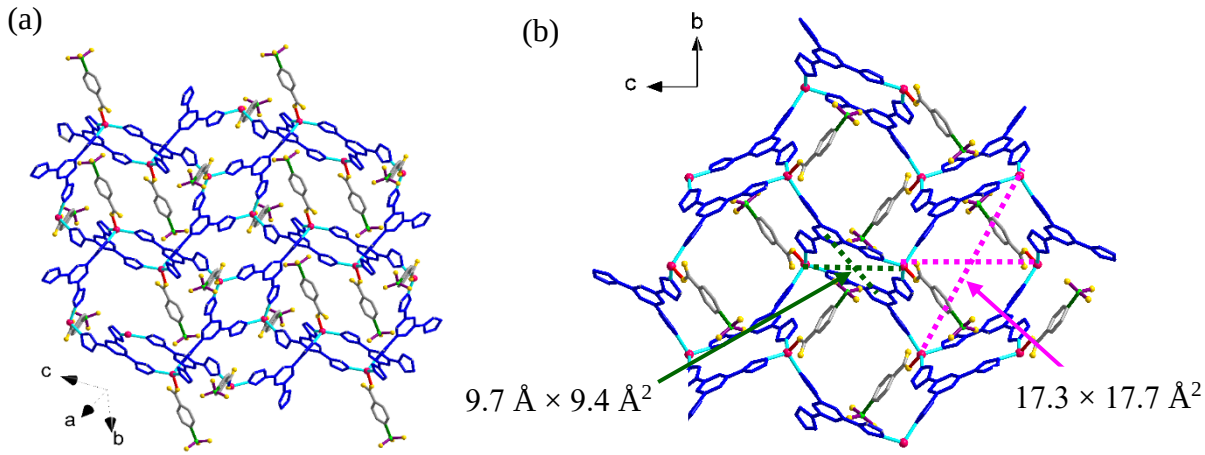

Fig. S9. Structures of **3**: (a) a view of 2D protuberant grid-layer; (b) having two types of pores with the window sizes of 17.3 × 17.7 Å^2 and 9.7 × 9.4 Å^2, respectively, excluded by the van der Waals radii of the atoms along the *a*-axis.

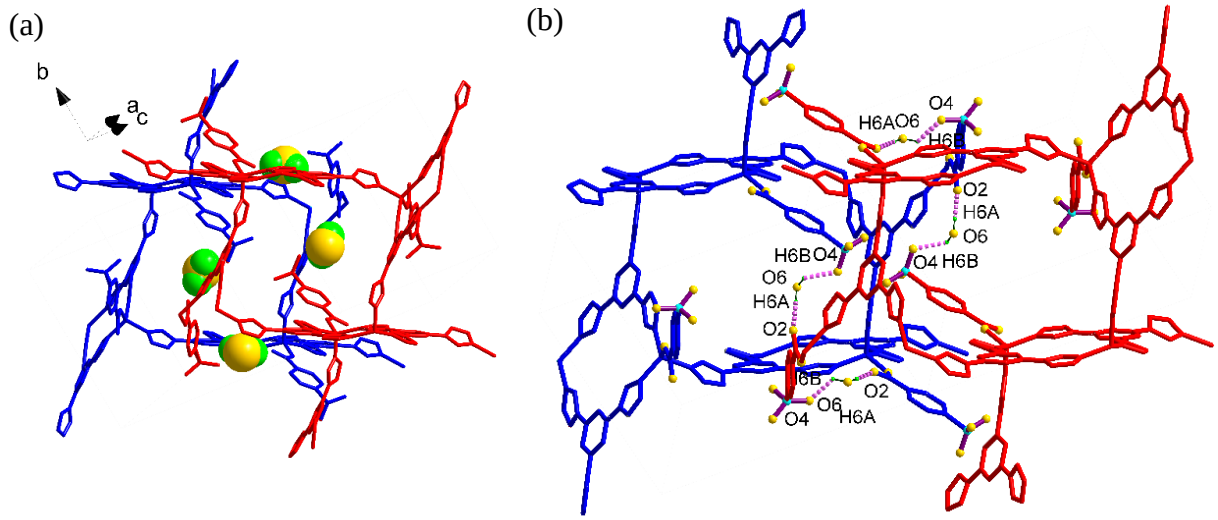

Fig. S10. Structures of **3**: (a) the guest aqueous molecules included within layers; (b) the hydrogen bonds are linked between the coordinated water molecules, the guest water molecules and DMF molecules, and the 4-sb^{2-} ligands.

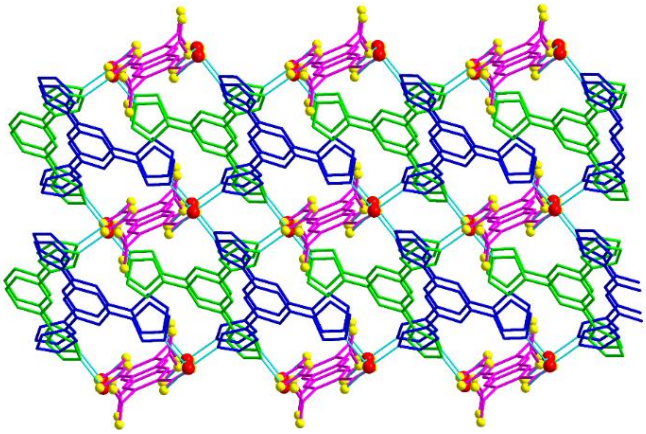

Fig. S11. The 2D layers of **4** are regularly stacked, yielding to the formation of a 3D framework.

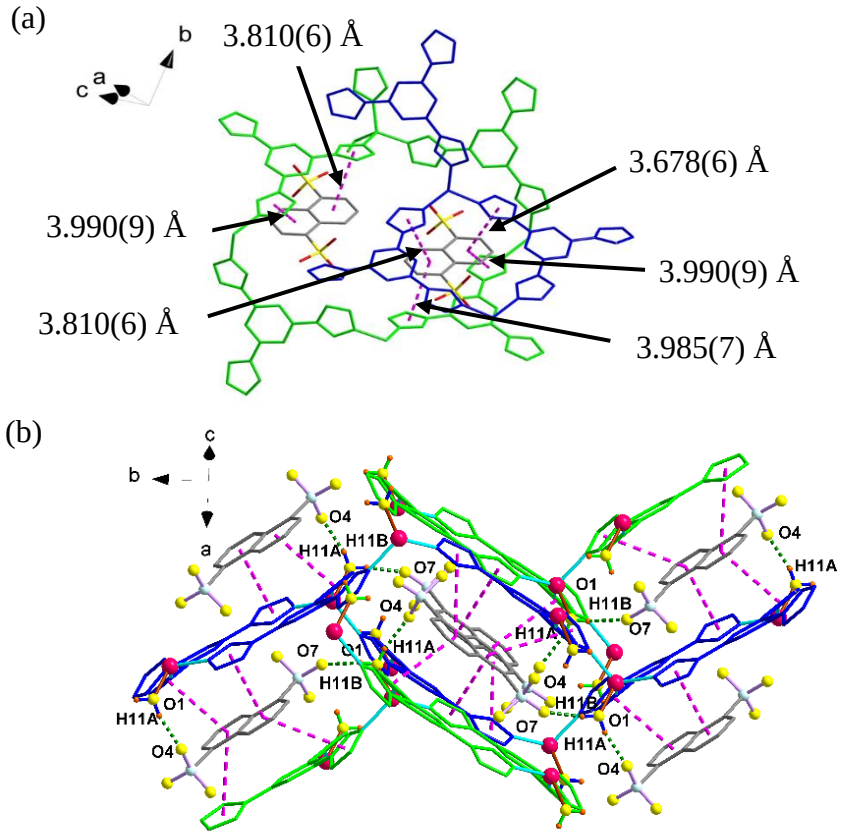

Fig. S12. Structures of **4**: (a) showing the neighboring layers are connected via the $\pi-\pi$ stacking interactions; (b) the abundant hydrogen bonding interactions present between the coordinated aqueous molecules and the guest 1,5-nds^{2-} anions.

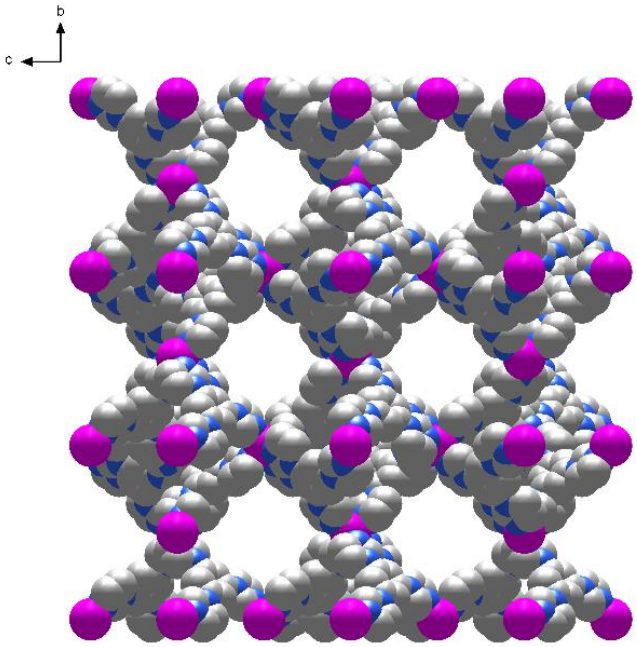

Fig. S13. Compound **5** contains the 1D channels with a window size of 16.3 × 16.3 $Å^2$ (excluded by the van der Waals radii of the atoms) in a space-filling mode along the *a*-axis.

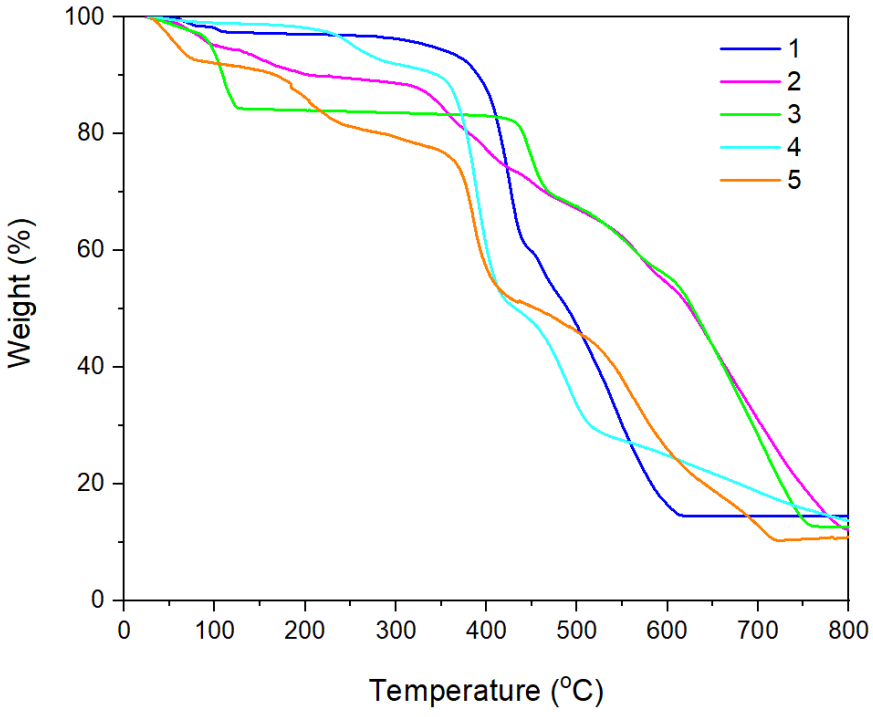

Fig. S14. TGA curves of **1**–**5**.

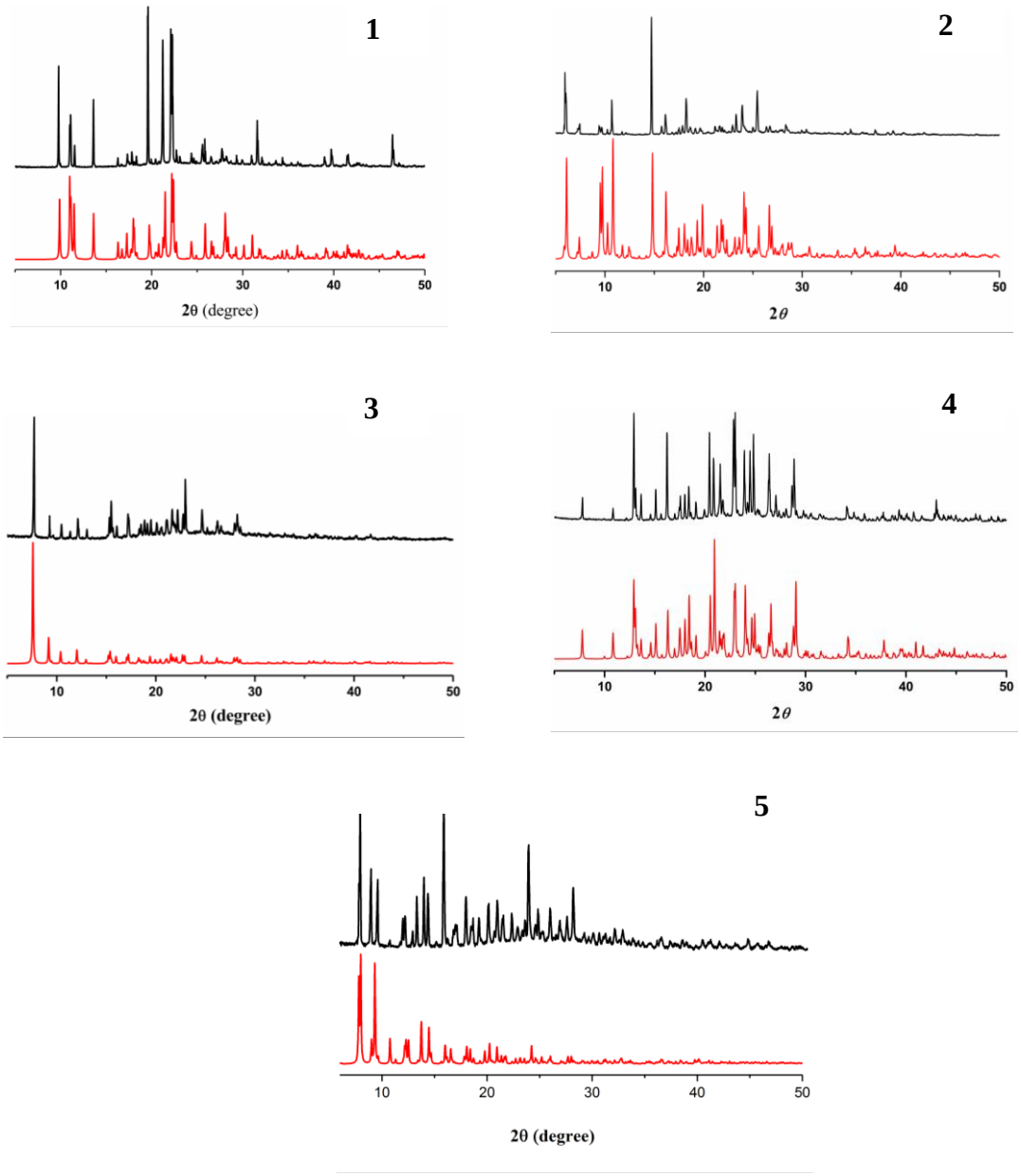

Fig. S15. As-synthesized (black) and simulated (red) powder X-ray diffraction patterns of **1**–**5**.

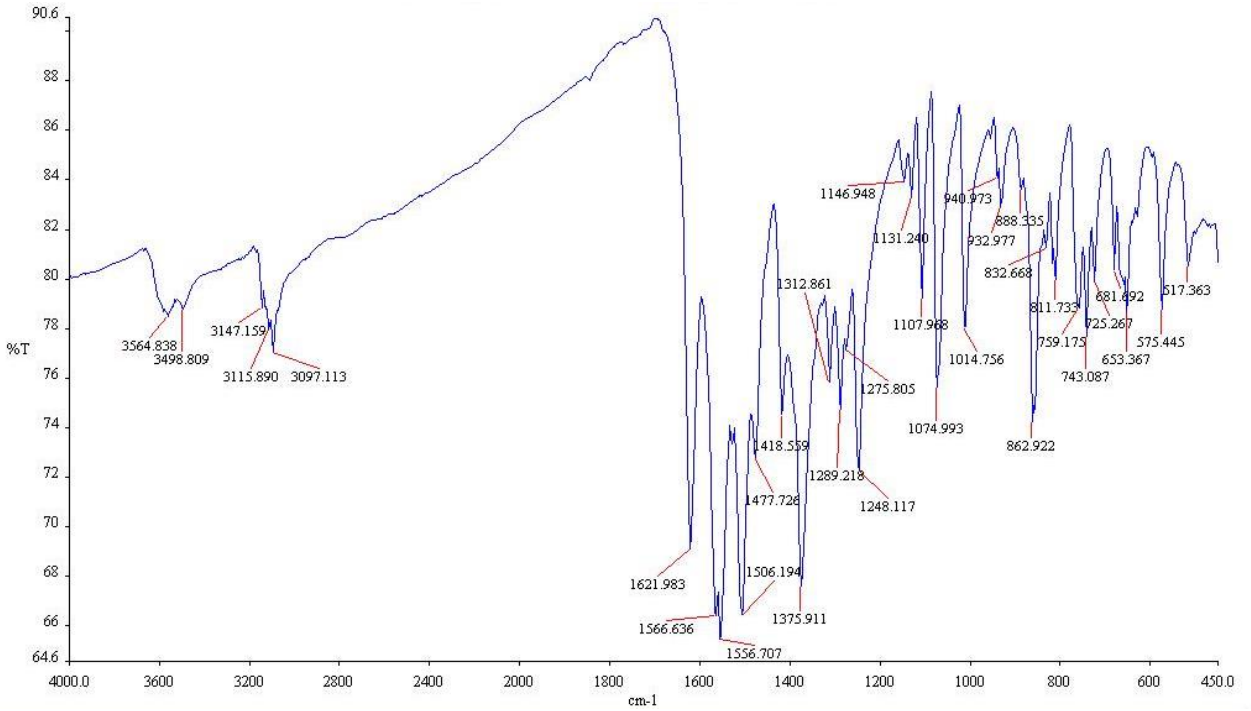

Fig. S16. FTIR spectrum of compound **1**.

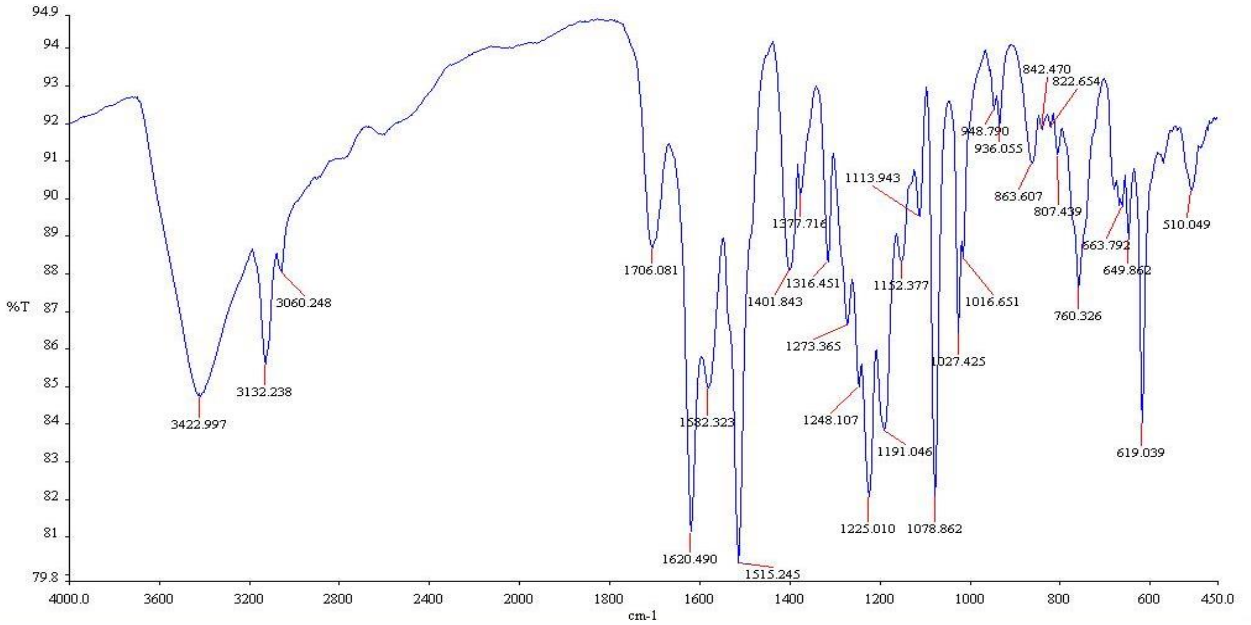

Fig. S17. FTIR spectrum of compound **2**.

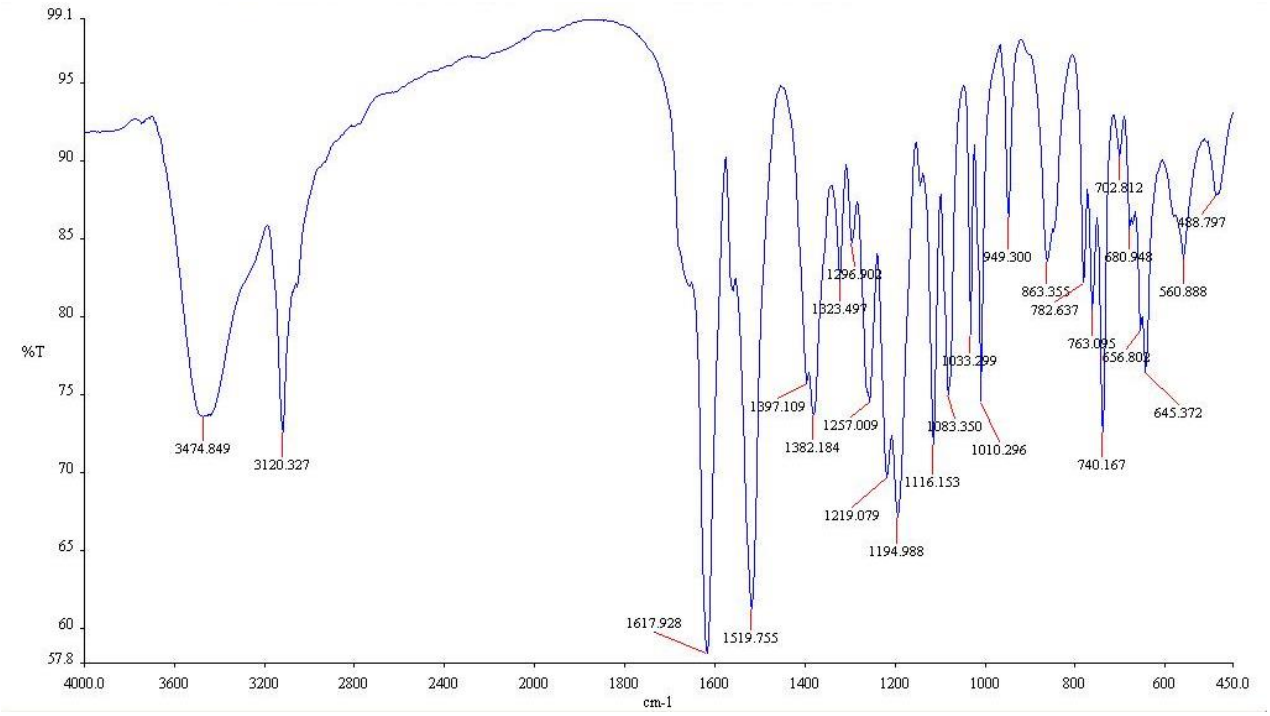

Fig. S18. FTIR spectrum of compound **3**.

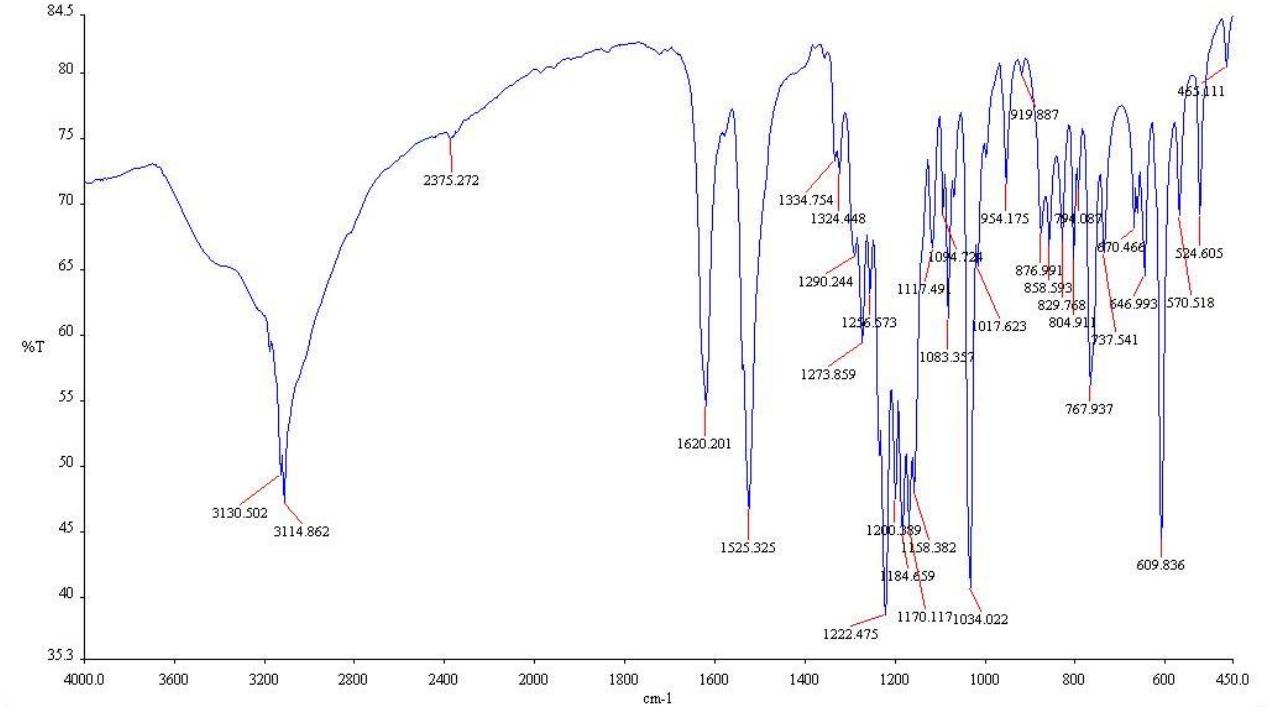

Fig. S19. FTIR spectrum of compound **4**.

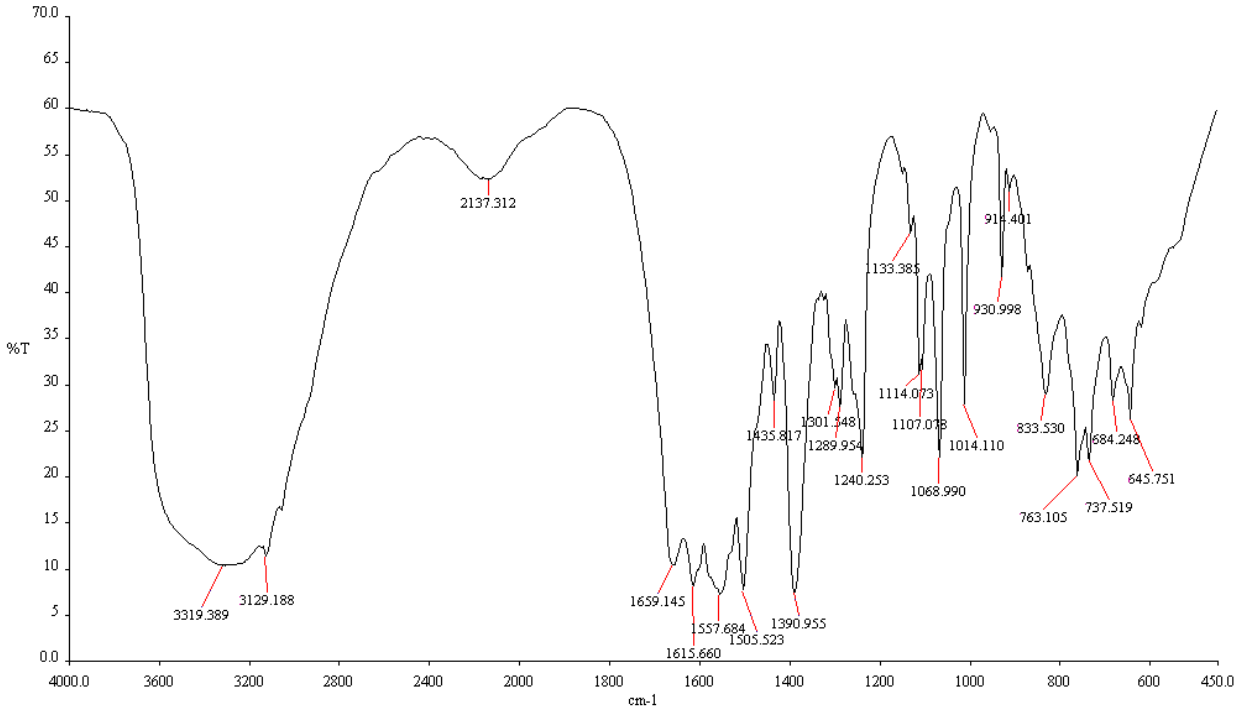

Fig. S20. FTIR spectrum of compound **5**.

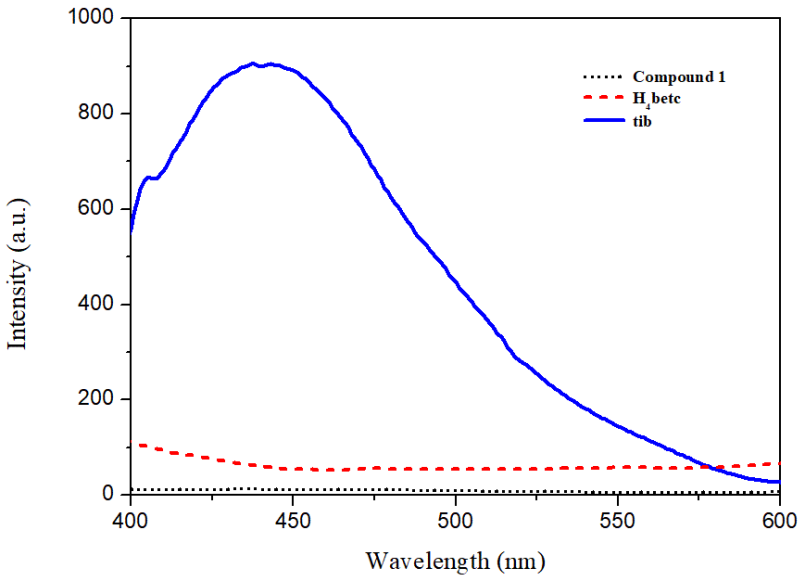

Fig. 21. The solid-state emission spectra of **1** shows at ca. 475 nm (λ_{ex} = 340 nm), tib ligand at 454 nm (λ_{ex} = 340 nm), and 1,2,4,5-benzenetetracarboxylic acid (H_4betc) at 470 nm (λ_{ex} = 380 nm).

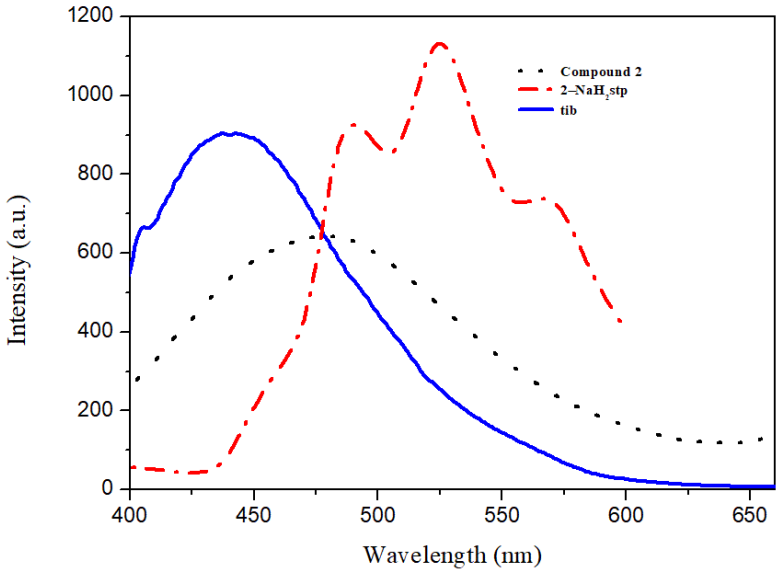

Fig. 22. The solid-state emission spectra of **2** shows at 480 nm (λ_{ex} = 360 nm), tib ligand at 454 nm (λ_{ex} = 340 nm), and monosodium 2-sulfoterephthalate (2-NaH_2stp) at 524 nm (λ_{ex} = 310 nm).

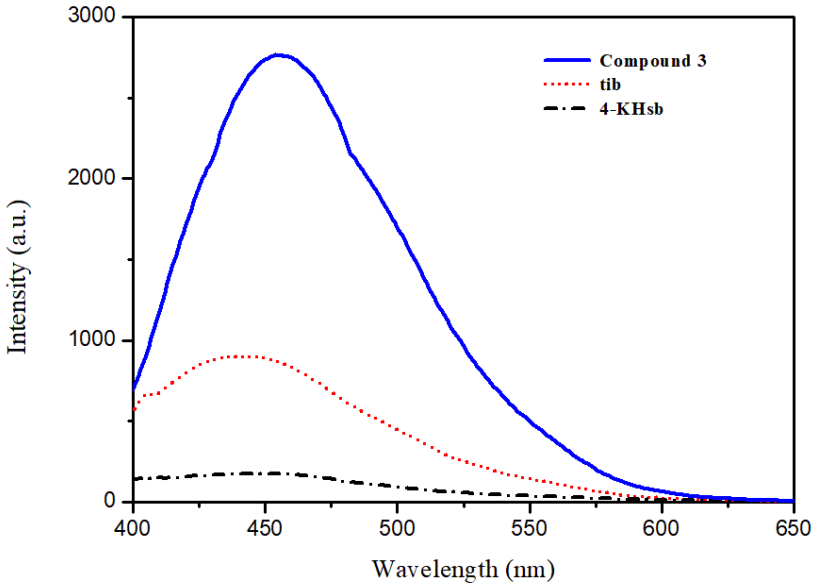

Fig. 23. The solid-state emission spectra of compound **3** shows at 458 nm (λ_{ex} = 340 nm), tib ligand at 454 nm (λ_{ex} = 340 nm), and potassium 4-carboxybenzenesulfonate (4-KHsb) at 455 nm (λ_{ex} = 350 nm).

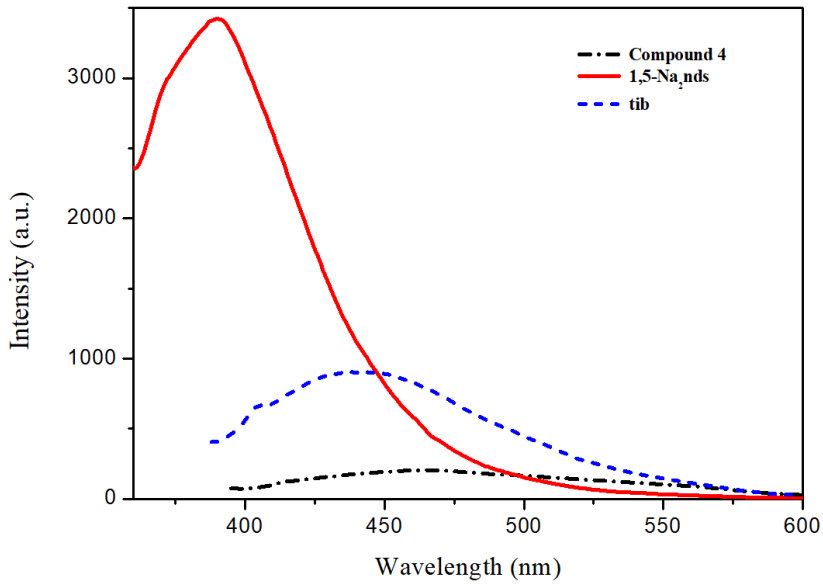

Fig. S24. The solid-state emission spectra of compound **4** shows at 467 nm (λ_{ex} = 380 nm), tib ligand at 454 nm (λ_{ex} = 340 nm), and 1,5-Na_2nds at 390 nm (λ_{ex} = 330 nm).

Table S1. The hydrogen bonding distance (Å) and angles (°) of **1**

D—H···A (Å)	**D—H (Å)**	**H···A (Å)**	**D···A (Å)**	**D—H···A (°)**
O(5)—H(5A)···O(1)	0.841(4)	2.096(3)	2.917(2)	165.0(3)
O(5)—H(6A)···O(1)	0.823(3)	2.695(2)	3.414(2)	146.9(3)
O(5)—H(6A)···O(3)	0.823(3)	2.675(4)	3.280(2)	131.7(3)

Table S2. The hydrogen bonding distance (Å) and angles (°) of **2**

D—H···A (Å)	**D—H (Å)**	**H···A (Å)**	**D···A (Å)**	**D—H···A (°)**
O(41)—H(41A)···O(9)	0.818(2)	1.746(2)	2.534(5)	161.2(6)
O(41)—H(41B)···O(1)	0.815(6)	2.950(7)	2.827(4)	106.5(6)
O(24)—H(24A)···O(15)	0.818(6)	2.993(8)	3.663(7)	140.7(6)
O(24)—H(24A)···O(16)	0.818(6)	1.834(6)	2.638(6)	167.8(7)

Table S3. The hydrogen bonding distance (Å) and angles (°) of **3**

D—H···A (Å)	**D—H (Å)**	**H···A (Å)**	**D···A (Å)**	**D—H···A (°)**
O(6)—H(6A)···O(2)	0.985(2)	1.944(2)	2.923(2)	178.5(1)
O(6)—H(6B)···O(4)	0.960(2)	2.126(4)	2.840(3)	130.2(6)

Table S4. The hydrogen bonding distance (Å) and angles (°) of **4**

D—H···A (Å)	**D—H (Å)**	**H···A (Å)**	**D···A (Å)**	**D—H···A (°)**
O(1)—H(11A)···O(4)	0.805(3)	1.849(3)	2.624(2)	161.5(2)
O(1)—H(11B)···O(7)	0.780(3)	1.861(4)	2.631(2)	168.5(2)

Table S5. Selected bond lengths [Å] and angles [°] for **1–5**

1					
Ni(1)−N(1)	2.059(2)	Ni(1)−N(5)	2.068(1)	Ni(1)−O(4)	2.149(2)
Ni(1)−N(3)	2.061(2)	Ni(1)−O(2)	2.063(2)	Ni(1)−O(3)	2.184(1)
N(3)−Ni(1)−O(2)	95.22(5)	N(3)−Ni(1)−N(5)	95.57(6)	N(1)−Ni(1)−O(4)	92.78(5)
N(1)−Ni(1)−N(5)	86.04(6)	O(2)−Ni(1)−N(5)	97.77(5)	N(3)−Ni(1)−O(4)	87.53(5)
N(1)−Ni(1)−O(3)	90.02(5)	N(3)−Ni(1)−O(3)	88.69(5)	O(4)−Ni(1)−O(3)	61.03(4)
N(1)−Ni(1)−N(3)	178.33(5)	O(2)−Ni(1)−O(4)	166.05(4)	N(5)−Ni(1)−O(3)	156.08(4)
N(1)−Ni(1)−O(2)	84.09(5)	N(5)−Ni(1)−O(4)	95.57(5)		
2					
Zn(1)−N(2)	2.178(5)	Zn(1)−O(36)	2.070(3)	O(39)-Zn(4)-N(22)	89.85(11)
Zn(1)−N(8)	2.025(3)	Zn(1)−O(8)	2.106(3)	O(39)-Zn(4)-O(40)	177.31(11)
Zn(2)−N(14)	2.151(3)	Zn(4)−O(1)	2.109(3)	O(39)-Zn(4)-N(26)	89.42(11)
Zn(2)−N(24)#2	2.174(3)	Zn(2)−N(4)	2.125(3)	O(40)-Zn(4)-N(10)	89.20(11)
Zn(3)−O(15)	1.938(3)	Zn(2)−N(18)#1	2.150(3)	N(28)-Zn(5)-N(12)#4	90.73(12)
Zn(3)−O(22)	1.940(3)	Zn(2)−O(38)	2.156(3)	N(28)-Zn(5)-N(12)	89.27(12)
Zn(4)−O(40)	2.154(3)	N(4)−Zn(2)−O(37)	92.58(12)	N(28)-Zn(5)-O(41)	91.74(12)
Zn(4)−N(10)	2.169(3)	O(38)−Zn(2)−O(37)	178.10(11)	N(12)-Zn(5)-O(41)	88.98(12)
Zn(5)−N(28)	2.108(3)	N(4)-Zn(2)-N(24)#2	87.42(12)	O(29)#5-Zn(6)-O(29)	127.4(2)
N(8)−Zn(1)−N(2)	113.65 (13)	O(15)-Zn(3)-N(20)	101.40(12)	O(29)-Zn(6)-N(30)#5	106.12(15)
N(2)−Zn(1)−O(8)	89.58(12)	N(16)-Zn(3)-N(20)	106.05(14)	N(30)-Zn(6)-N(30)#5	110.9(2)
3					
Zn(1)−N(1)	2.000(2)	Zn(1)−N(6)	1.987(2)	O(1)−Zn(1)−N(1)	107.91(10)
Zn(1)−N(4)	1.988(2)	Zn(1)−O(1)	1.934(2)	N(4)#4−Zn(1)−N(1)	108.2(1)
N(6)#3−Zn(1) −N(4)#4	116.4(1)	N(6)#3-Zn(1)-N(1)	109.06(9)	O(1)−Zn(1)−N(6)#3	101.6(1)
O(1)−Zn(1)−N(4)#4	113.2(1)				
4					
Zn(1)−N(4)	1.965(2)	Zn(1)−N(6)	1.970(2)	N(4)−Zn(1)−O(1)	108.35(8)
Zn(1)−O(1)	1.967(2)	Zn(1)−N(1)	2.004(2)	N(4)−Zn(1)−N(6)	116.51(7)
O(1)−Zn(1)−N(1)	104.39(8)	N(6)−Zn(1)−N(1)	111.14(7)	O(1)−Zn(1)−N(6)	103.25(8)
N(4)−Zn(1)−N(1)	112.05(7)				
5					
Zn(1)−N(1)	1.976(4)	N(1)−Zn(1)−N(1)#3	102.4(3)	N(1)−Zn(1)−N(1)#4	113.14(17)
N(1)#3−Zn(1)−N(1)#4	113.14(17)				

[a]Symmetry transformations used to generate equivalent atoms, for **2** : #1 –x + 1, –y + 2, –z + 2; #2 x, –y + 2, z + 1/2; #4 –x, –y + 2, –z + 1; #5 –x, y, –z + 1/2; for **3**: #3 –x + 1/2, y – 1/2, –z + 3/2; #4 x + 1/2, –y + 3/2, z + 1/2; for **5**: #3 –x + 5/4, y + 0,–z + 5/4; #4 –z + 5/4, –y + 3/4, x.